Brain oscillatory modes as a proxy of stroke recovery

Authors:

Sylvain Harquel, PhD[1, 2,†]; Andéol Cadic-Melchior, MS[1, 2,†]; Takuya Morishita, PhD[1, 2]; Lisa Fleury, PhD[1,2]; Martino Ceroni, MS[1, 2]; Pauline Menoud, MS[1, 2]; Julia Brügger, PhD[1, 2]; Elena Beanato, MS[1, 2]; Nathalie H. Meyer, MS[3]; Giorgia G. Evangelista, PhD[1, 2]; Philip Egger, PhD[1, 2]; Dimitri Van de Ville, PhD[4, 5]; Olaf Blanke, PhD [3,8]; Silvestro Micera, PhD[6, 7]; Bertrand Léger, PhD[9]; Jan Adolphsen, MD[10]; Caroline Jagella, MD[11]; Andreas Mühl, MD[9]; Christophe Constantin, MD[12]; Vincent Alvarez, MD[12]; Philippe Vuadens, MD[9]; Jean-Luc Turlan, MD[9]; Diego San Millán, MD[12]; Christophe Bonvin, MD[12];Philipp J. Koch, MD[1, 2,13]; Maximilian J. Wessel, MD[1, 2,14]; and Friedhelm C. Hummel, MD[1, 2,15*]

† These authors contributed equally to this work.

Affiliations:

[1] Defitech Chair of Clinical Neuroengineering, Neuro-X Institute (INX) and Brain Mind Institute (BMI), École Polytechnique Fédérale de Lausanne (EPFL), 1202 Geneva, Switzerland
[2] Defitech Chair of Clinical Neuroengineering, INX and BMI, EPFL Valais, Clinique Romande de Réadaptation, 1950 Sion, Switzerland
[3] Laboratory of Cognitive Neuroscience, INX and BMI, EPFL, 1202 Geneva, Switzerland
[4] Medical Image Processing Laboratory, INX, EPFL, 1202 Geneva, Switzerland
[5] Department of Radiology and Medical Informatics, University of Geneva (UNIGE), 1205 Geneva, Switzerland
[6] The Biorobotics Institute and Department of Excellence in Robotics & AI, Scuola Superiore Sant'Anna, Pisa, Italy
[7] Bertarelli Foundation Chair in Translational Neuroengineering, INX and Institute of Bioengineering, School of Engineering, Ecole Polytechnique Fédérale de Lausanne
[8] Department of Neurology, Geneva University Hospital (HUG), 1205 Geneva, Switzerland
[9] Clinique Romande de Réadaptation, 1950 Sion, Switzerland
[10] Mediclin Reha-Zentrum Plau am See, 19395 Plau am See, Germany
[11] Berner Klinik Montana, 3963 Crans-Montana, Switzerland
[12] Department of Neurology, Hôpital du Valais, 1950 Sion, Switzerland
[13] Department of Neurology, University of Lübeck, Lübeck, Germany
[14] Department of Neurology, Julius-Maximilians-University Würzburg, Würzburg, Germany
[15] Clinical Neuroscience, Geneva University Hospital, Geneva, Switzerland

*Corresponding author:
Prof. Dr. Friedhelm C. Hummel
Defitech Chair of Clinical Neuroengineering
Neuro-X Institute (INX) and Brain Mind Institute
École Polytechnique Fédérale de Lausanne (EPFL)
9 Chemin des Mines, 1202 Geneva, Switzerland
and
École Polytechnique Fédérale de Lausanne (EPFL Valais)
Clinique Romande de Réadaptation
Av. Grand-Champsec 90,
1951 Sion
Email: friedhelm.hummel@epfl.ch
Telephone: +41 21 69 35 440

Abstract:

Background and Objectives: Stroke is the leading cause of long-term disability, making the search for successful rehabilitation treatment one of the most important public health issues. A better understanding of the neural mechanisms underlying impairment and recovery and the development of associated markers is critical for tailoring treatments to each individual patient with the ultimate goal of maximizing therapeutic outcomes.

Methods: Here, we used a novel and powerful method consisting of combined transcranial magnetic stimulation (TMS) and multichannel electroencephalography (EEG) to analyze TMS-induced brain oscillations in a large cohort of 60 stroke patients from the acute to the early-chronic phase after a stroke.

Results: A data-driven parallel factor analysis (PARAFAC) approach to tensor decomposition allowed to detect brain oscillatory modes specifically centered on the θ, α and β frequency bands, which evolved longitudinally across stroke stages. Notably, the observed modulations of the α-mode, which is known to be linked with GABAergic system activity, were associated to the extent of motor recovery.

Discussion: Overall, these longitudinal changes provide novel insights into the functional reorganization of brain networks after a stroke and its underlying mechanisms. Notably, we propose that the observed α-mode decrease corresponds to a beneficial disinhibition phase between the subacute and early-chronic stage that fosters structural and functional plasticity and facilitates recovery. Monitoring this phenomenon at the individual patient level will provide critical information for phenotyping patients, developing electrophysiological biomarkers and refining therapies based on personalized excitatory/inhibitory neuromodulation using noninvasive or invasive brain stimulation techniques.

INTRODUCTION

Stroke is the leading cause of motor disability in the adult population. The exact mechanisms underlying motor impairment and recovery are the targets of a relentless search *(1–4)*, but have yet to be elucidated in detail. Mechanistic knowledge is critical for designing and optimizing future patient-tailored rehabilitation protocols, in contrast to the current "one-size-fits-all" strategy adopted with limited success *(5–7)*. Among the proposed mechanisms, the role of the inhibitory system within the ipsilesional hemisphere has been suggested to be crucially relevant for the course of stroke recovery *(8–10)*. Indeed, modulation of inhibition processes can be either beneficial or detrimental for recovery, depending on its direction (increase or decrease) and exact timing. While an increase of the gamma-aminobutyric acid (GABAergic) system activity is beneficial for limiting excitotoxic cell death in the hyper-acute stage, its lasting is detrimental and the presence of a disinhibition phase in later stages is instead favorable for fostering structural plasticity *(10)*. However, such phenomena have so far only been examined in animal models or small cohorts of mildly impaired patients *(8, 9, 11–13)*. In the present work, we monitored it longitudinally in a cohort of stroke patients, by focusing on brain oscillations induced by non-invasive cortical stimulation, using the coupling between scalp electroencephalography (EEG) and transcranial magnetic stimulation (TMS).

TMS-EEG coupling offers the unique opportunity to directly probe the properties of the neuronal electrophysiological activity *(14)*. It inherits both from the causal inference *(15)* and the spatial resolution of TMS *(16)*, and from the temporal resolution of EEG, which allows to directly study neuronal oscillations. Since TMS pulses mainly act as a phase reset on neural oscillators *(17, 18)*, this tool allows to better characterize the brain dynamics, i.e., evoked neural oscillatory activity, of an area *(19, 20)*. Such readouts might be markers of functional reorganization processes that

enable motor recovery, especially among the thalamocortical networks to which this technique is sensitive *(20, 21)*. Focusing on *evoked* – instead of *induced* - oscillations excludes nonstationary brain activity *(18, 22)*, thus eliminating all sources of variability regarding oscillation latency and phase from one stimulation to another *(17, 18)*. In a seminal study with healthy subjects, Premoli *et al. (26)* explored TMS-induced oscillations over M1 and found specific patterns of oscillations in the α and ß bands. Furthermore, the authors revealed a link between these patterns and the modulation of the GABAergic inhibitory system activity, which is of particular interest in the context of this study.

Recent studies proposed the use of a data-driven approach, the parallel factor analysis (PARAFAC) *(24)*, capable of reducing the complexity inherent to TMS-induced oscillations datasets, which are multidimensional (3-5D), into a simpler collection of parsimonious and unique components, or modes *(25, 26)*. Applied on TMS-EEG datasets, it allowed to extract three to four brain oscillatory modes in M1 that were physiologically meaningful *(25, 26)*.These modes did not overlap in frequency; instead, each was primarily driven by one main oscillatory pattern in the θ, α or β band, each related to a specific mechanism. The first θ-band mode might well be the signature of feedback from remote areas engaged after the indirect activation of cortico-cortical and cortico-subcortical networks *(27, 28)*, since this low-frequency band has been associated with interregional communication supporting cognition in humans and animals *(29–31)*. Its study is of interest here, given the fact that such phenomena are heavily impacted in brain network diseases like stroke *(2, 32)*. The study of the second mode that focused on late TMS-induced α oscillations is what allows to monitor the evolution of inhibitory processes in the time course of post-stroke motor recovery, since variations within this band are linked with functional inhibitory processes *(33–38)* mediated by the GABAergic system *(23)*.

In the present study, we sought to elucidate the mechanisms underlying motor impairment and recovery after stroke by applying this powerful method in a large stroke cohort evaluated longitudinally from the acute to the chronic stage, in the framework of the TiMeS project *(39)*. The present work complements the study of TMS-evoked response *(40)*, the results of which will be put into perspective with those of the present study. Here, we specifically studied the changes in brain oscillatory modes unveiled from TMS-induced oscillations and determined their importance for residual motor functions and recovery.

MATERIALS AND METHODS

This work is part of the TiMeS project, a detailed description of which is provided in Fleury *et al.,* 2022, and in the Supplementary online materials.

Study design

TMS-induced oscillations and behavior were assessed at three different time points, one week (referred to here as "acute stage", A), three weeks ("subacute stage", SA) and three months poststroke ("early-chronic stage", EC, Fig. 1A). Seventy-six stroke patients participated in the study after being admitted to the Regional Hospital of Sion (HVS), Switzerland. Among them, 60 (age: 66.9 ± 13.3 years; 18 females) were included in this study, i.e., patients with TMS-EEG recordings at least in the first recording session (A stage). Additionally, 19 healthy young adults (age: 26.9 ± 2.9 years, 9 females) and 15 healthy old adults (aged-matched with patients, age: 67 ± 5 years, 11 females) were recruited and underwent a single TMS-EEG recording session. The study was conducted in accordance with the Declaration of Helsinki and was approved by Cantonal

Ethics Committee Vaud, Switzerland (project number: 2018-01355). Written informed consent was obtained from all participants.

Behavioral data

At each time point, the bilateral motor capability (and impairment) of patients were assessed using (i) the Fugl-Meyer Assessment (FM) of the upper limb (FM-UL, without reflexes), of the upper extremity (FM-UE), of the hand and of the wrist *(41)*, (ii) the maximum fist, key and pinch force, (iii) the box and blocks test (BnB), and (iv) the nine-hole peg test *(42)*. Change ratios between time points were computed for each motor measurement x as follows (e.g., A vs. SA): $(x_{SA} - x_A)/x_A$.Patients were classified as "recovering" if they exhibited an improvement in FM-UE scores from the A stage to the SA stage or from the A/SA stages to the EC stage.

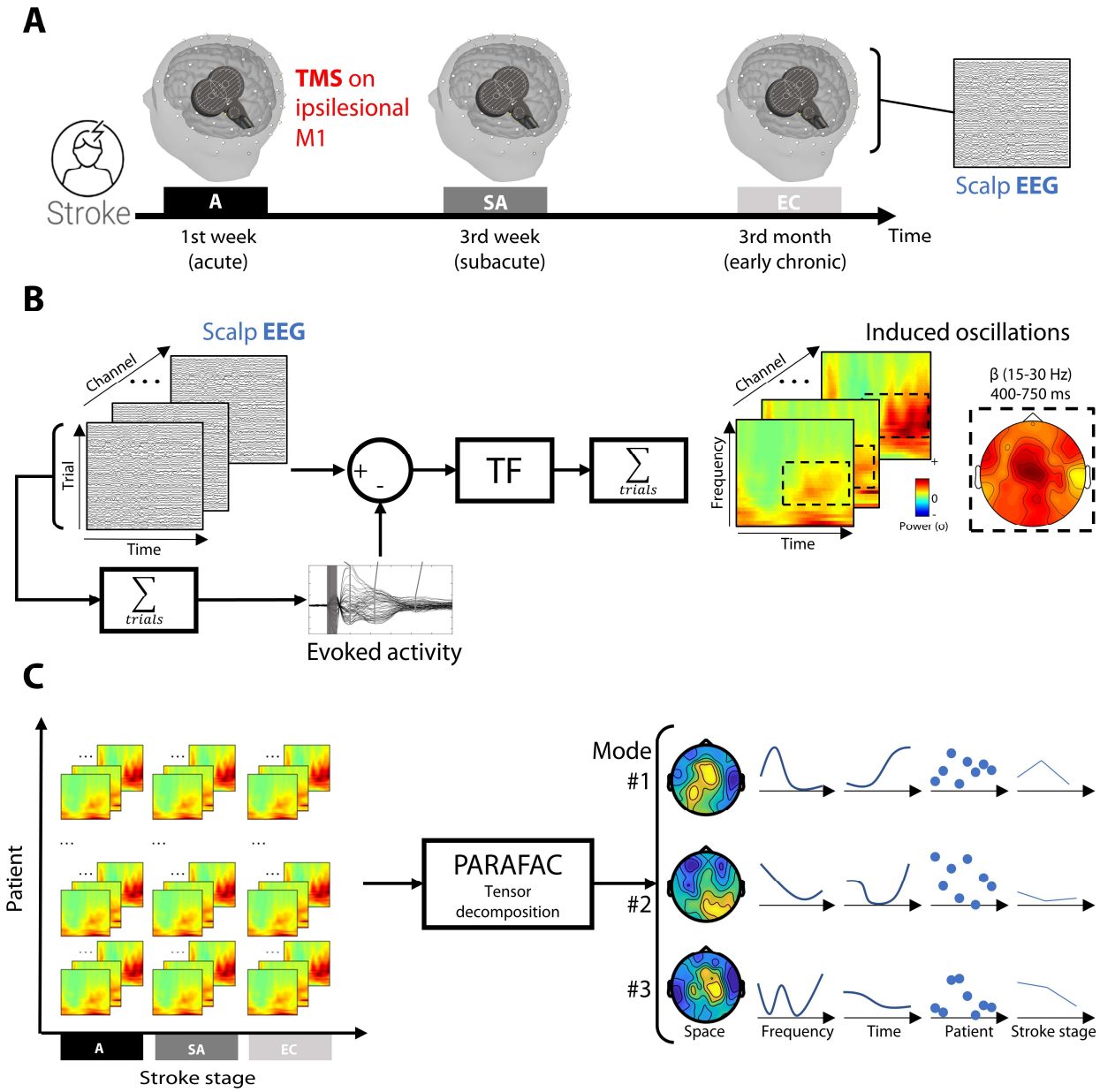

Fig. 1: Protocol design and main data processing pipeline. (**A**). Protocol design including 3 TMS-EEG coupling sessions during the 1st week, 3rd week and 3rd month after stroke (referred to as the acute, subacute and early-chronic stages, respectively). (**B**). Signal processing pipeline for computing induced oscillation maps. For each patient and channel, the evoked activity (average of the clean signal across trials) was removed from the clean signal prior to the time-frequency (TF) transform. Each TF map was z transformed with baseline values (-200 to -50 ms prior to TMS pulse) before averaging across trials. Examples of induced oscillation maps (+40 to +750 ms; 7 to 40 Hz) and the topography of late central β oscillations are depicted on the right for one representative patient. (**C**). Tensor decomposition using the PARAFAC approach. Induced oscillation maps were compiled into a tensor, with the patient and stroke stages as the 4th and 5th dimensions, respectively, and decomposed using the PARAFAC algorithm. This decomposition

led to several components, or modes, whose weights are represented in the space (topography), frequency, time, patient and stroke-stage dimensions, from left to right.

TMS-EEG analysis

The analysis methodology used in this study was adapted from Tangwiriyasakul *et al. (35)*, in which the PARAFAC tensor decomposition approach was applied to TMS-EEG data.

Preprocessing

TMS-EEG data were analyzed with MATLAB (The MathWorks, USA) and preprocessed using the EEGLAB *(43)* and TESA *(44)* toolboxes. The clean datasets analyzed in this study were identical to those in our previously published paper *(40)*. In short, raw TMS-EEG data were preprocessed using a double independent component analysis (ICA) *(45)* to remove components linked to pulse, muscle, decay and ocular artifacts from the data. The preprocessed dataset resulted in an average of 149 ± 24 cleaned trials epoched from -500 to +1,000 ms around the TMS pulse and filtered between 1 and 80 Hz.

Induced oscillations

Induced oscillations were computed in MATLAB using the Fieldtrip toolbox *(46)* (Fig. 1B). First, the TMS-evoked potentials (TEPs) were computed by averaging all trials and were then individually subtracted from the signal in each trial to filter out evoked activity *(47)*. Then, the time-frequency (TF) map of each corrected trial was computed using a multitapers approach. The signal from the -500 to +1,000 ms time window (10-ms step) was convoluted with Hanning tapers ranging from 7 to 40 Hz (1-Hz step), with a width of 3.5 cycles per window. For each electrode and trial, the resulting power time series was normalized using the z-score against baseline (-200 to -50 ms), before being averaged across trials to obtain the final TF maps. Prior to tensor

definition, all the TF maps were flipped as needed so that the ipsilesional hemisphere was defined as the left for all patients.

PARAFAC tensor decomposition

Four different tensors were constructed to answer the study's main questions as follows: the first tensor focused on the A stage (4D: electrode × frequency × time × patient), while the second to the fourth tensors gathered the induced oscillations across stroke stages (A vs. SA stage, A vs. EC stage, and from A to EC stage; 5D: electrode × frequency × time × patient × stroke stage) (Fig. 1C). For each tensor, the TF maps were cropped between +40 and +750 ms to prevent missing values from boundary effects, resulting in a size of 62 × 34 × 70 for the first three dimensions. The fourth dimension size was equal to the number of patients included at the A stage (60), the A and SA or EC stages (43 or 33 respectively), and all stages (27).

Statistical analysis

Differences between stroke stages when decomposing the 5D tensors were assessed using the same permutation-based approach proposed in *(25)*. In short, 1,000 surrogate tensors were obtained by permuting data from the 4th (patient) and 5th (stroke stage) dimensions while keeping the data structure unchanged over the 3 first dimensions. A PARAFAC decomposition was then performed on each surrogate tensor using the old loadings of the original data decomposition in the first three dimensions. The corresponding mean differences between stroke stages were gathered across all decompositions to form the surrogate data distributions. Differences between stroke stages within each brain mode (θ, α and β modes) in the original tensors were considered significant if greater or lower than 2.5% of these surrogate distributions ($p < 0.05$, two-sided). This alpha level was Bonferroni corrected in order to account for multiple testing (1 or 3 differences × 3 modes = 3 or

9, for tensors including 2 or 3 stroke stages respectively), which led to a corrected threshold of 0.83% or 0.25% respectively (referred as $p_{Bonf} < 0.05$ in the text).

The link between patient weights (data in the 4th dimension) within the extracted modes and motor scores (see *Behavioral data*) was explored using the Bayesian equivalent of nonparametric Kendall correlation and partial correlation testing using JASP software (JASP Team - 2022). The weights of each extracted mode were compared with the initial motor scores in the A stage and to the change ratio between stroke stages (see *Behavioral data*). The default values proposed within the JASP framework were used to keep the priors regarding effect sizes relatively large. Correlation values were reported using the 95% confidence interval of Kendall's τ, while the statistical evidence of the tests was reported using Bayes factors (BF_{10}) and the cutoff values defined by Jeffreys (1998) for interpretation.

RESULTS

All 60 patients, whose characteristics are detailed in Table 1, underwent longitudinal TMS-EEG evaluations without any adverse events. The lesion heatmap of the patient cohort at inclusion is depicted in Fig. 2. Overall, patients recovered from their stroke-induced motor impairment from the acute to the early-chronic stages, exhibiting average reductions in motor impairment of 7.7 points on the FM–UE.

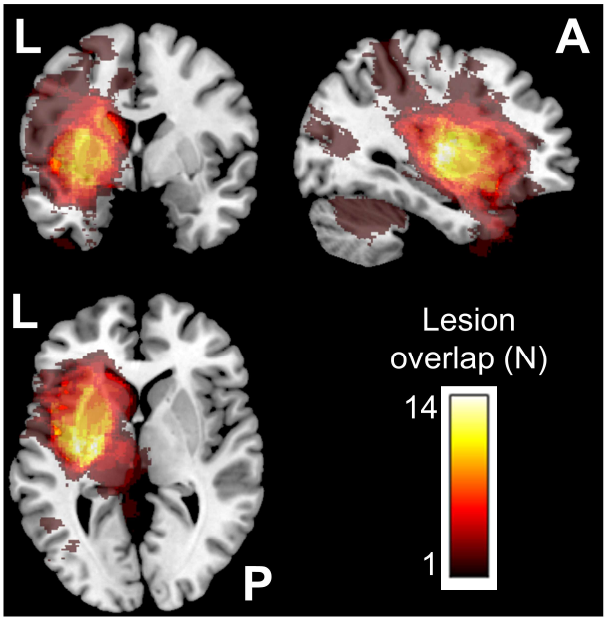

Fig. 2: Lesion heatmap of patients at the acute (or subacute, if data unavailable) stage, N = 54. Right-hemispheric lesions were flipped to the left side. Note that 6 out of 60 patients did not undergo magnetic resonance imaging (MRI) at the acute or subacute stages.

Table 1: Patient characteristics.

Sex	Age (years)	Handedness	Hemisphere affected	Resting Motor Threshold (% MSO)	Days poststroke			FM–UE score (/60)			NIHSS score		
				Acute	Acute	Subacute	Early-chronic	Acute	Subacute	Early-chronic	Acute	Subacute	Early-chronic
18 F/ 42 M	66.9 ± 13.3	54 right-handed	30 Left/ 30 right	43 ± 10	6.6 ± 2.3	27 ± 5	98.6 ± 8.8	47.3 ± 18.5	50.9 ± 16.5	55 ± 12.1	5.7 ± 5.4	2.0 ± 3.0	0.6 ± 1.3

MAS score (/48)			MoCA score (/30)			Barthel Scale score (/100)			Box and blocks test score (aff./nonaff.)			Nine-hole peg test score (aff./nonaff.)		
Acute	Subacute	Early-chronic	Acute	Subacute	Early-chronic	Acute	Subacute	Early-chronic	Acute	Subacute	Early-chronic	Acute	Subacute	Early-chronic
3 ± 5.6	2.5 ± 4.9	1.3 ± 2.4	22.7 ± 4.9	24.1 ± 4.9	25.9 ± 3.5	88.2 ± 19.5	93.8 ± 13	99 ± 3.1	0.74 ± 0.34	0.79 ± 0.31	0.89 ± 0.23	2.6 ± 2.4	2.1 ± 2.2	1.6 ± 1.6

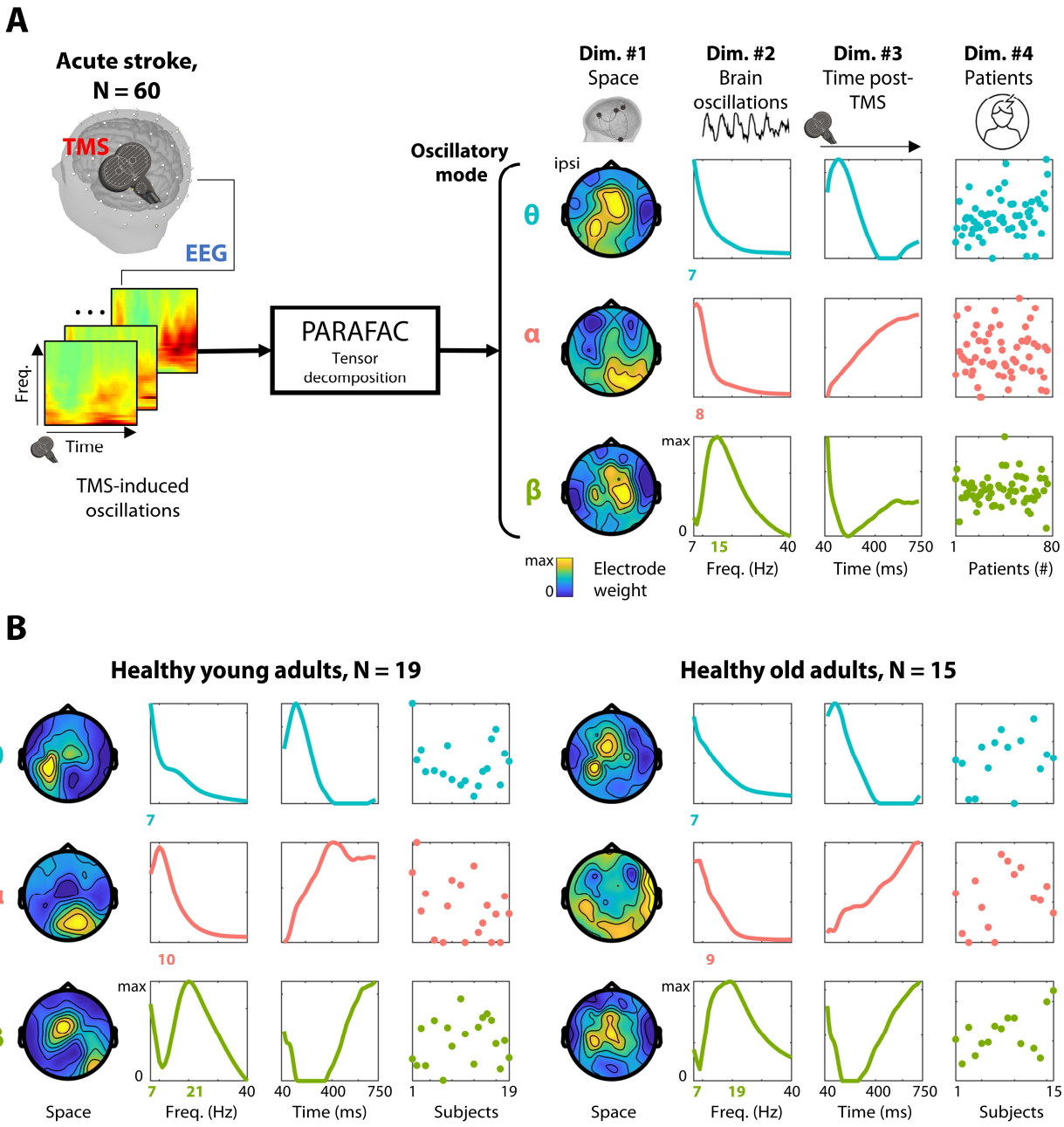

Fig. 3: Brain oscillatory modes extracted from stroke patients and healthy adults. (**A**) PARAFAC decomposition of the 4D tensor of the TMS-induced oscillations in acute stroke patients. Modes are sorted by row according to their main frequency peak, from θ (7 Hz, blue) and α (8 and 10 Hz, red) to high β (15 and 21 Hz, green) frequency bands (top to bottom). Each column depicts the relative weights (from 0 to maximum) of each mode in the space, frequency, time and patient dimensions (from left to right). The mode frequency peak is highlighted in color on the y-axis. Data were flipped for patients whose lesion was located on the right hemisphere so that the ipsilesional side was the left side. (**B**) Results of the same tensor decomposition in healthy young (left) and old (right) adults, with similar sorting of modes.

Perturbation of brain oscillatory modes in acute stroke patients

Fig. 3 shows the induced oscillatory modes obtained after the 4D tensor decomposition in A patients and in healthy groups The three identified modes were similar among the three groups; however, the three decompositions pointed toward an overall slowdown of brain oscillatory activity in A patients, indicated by a decrease in the peak frequency of the different modes. The first mode was centered on θ oscillations (7-Hz peak) distributed over the stimulation site. The second mode converged on the late parieto-occipital α waves that emerged over time starting 150-200 ms after stimulation. The main frequency of this mode tended to be lower in A patients (8 Hz) than in healthy young (10 Hz) and aged-match older adults (9 Hz). The third mode mainly focused on central sensorimotor β and μ waves. The peak frequency tended to differ among the three groups: A patients presented one peak at 15 Hz, while healthy young adults showed two peaks at 7 and 21 Hz, and older adults showed one peak at 19 Hz.

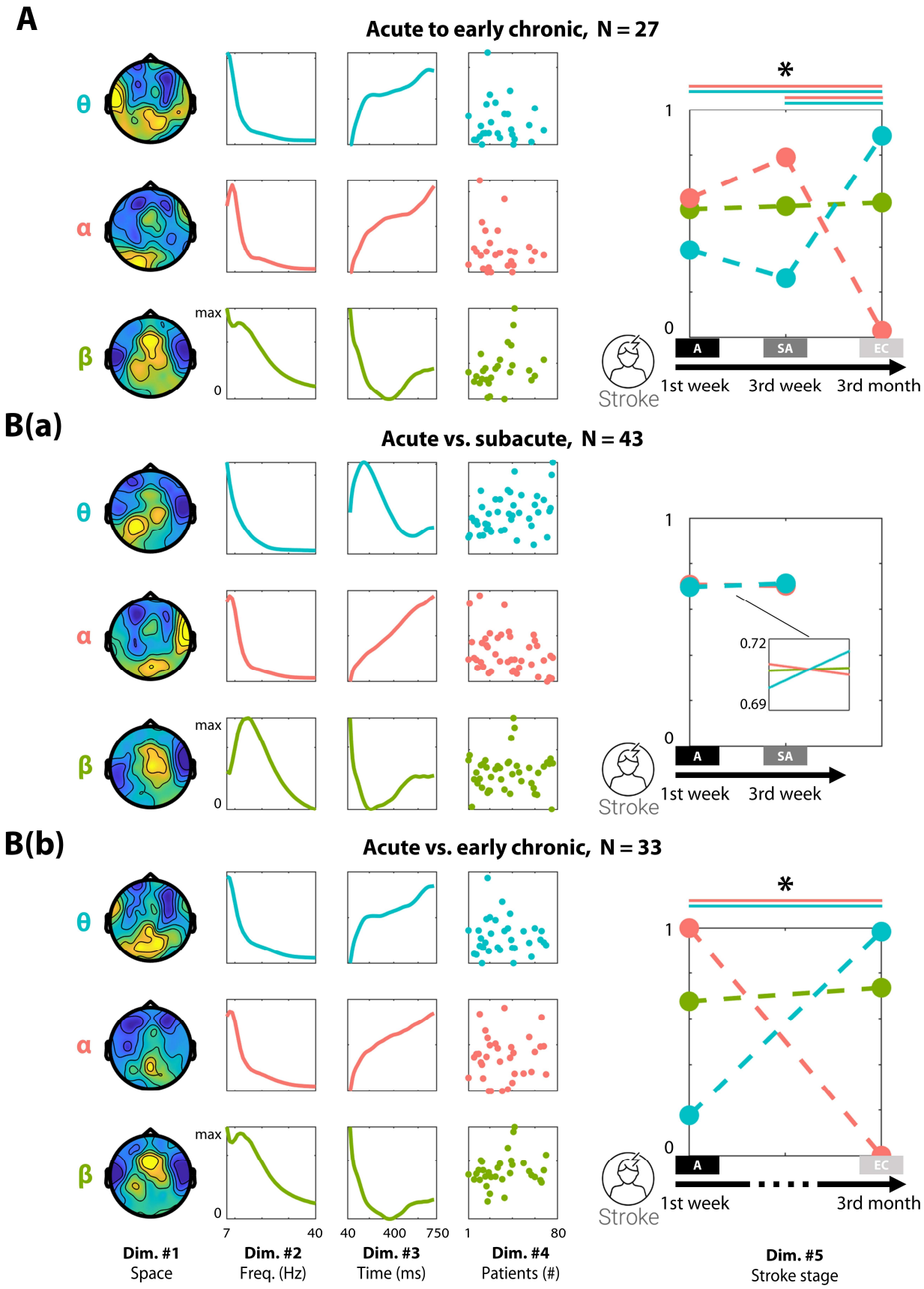

Fig. 4: **Evolution of brain oscillatory modes from acute to early-chronic stages**. (**A**) PARAFAC decomposition of the 5D tensor in all patients leading to 3 main modes. The modes are sorted by peak frequency, from θ (blue) and α (red) to β (green) bands. Each column depicts the relative weights (from 0 to maximum) of each mode in the space, frequency, time, patient and stroke-stage dimensions (from left to right). The asterisk and colored lines indicate significant effects of the pairwise comparisons of the stroke stages within the θ (blue lines) and α (red lines) modes for the acute (A) vs. early-chronic (EC) stages and the subacute (SA) vs. early-chronic (EC) stages (permutation test, $p_{Bonf} < 0.05$, see *Statistical analysis*). (**B**). The results of the same decomposition, run separately on the A and SA stages **(a)** and on the A and EC stages **(b)**. Note that mode weights overlap on the y-axis (0-1 scale) for A vs. SA (**B(a)**). Taken together, the results indicate that there were changes in the θ and α-band modes over time, especially large changes in the θ and α-band modes from A to EC, but no changes in the β-band mode in general.

Evolution of brain oscillatory modes over the time course of recovery

The results of the decomposition of the 5D tensors including all stroke stages (A, SA and EC) are presented in Fig. 4. Interestingly, the mode weights were significantly modulated across stroke stages ($p_{Bonf} < 0.05$, see Fig. S1 for detailed results). This change was specific to α- and θ-band modes that significantly differed from the A and the SA stages to the EC stage with opposite directions. While the relative weight of the α-band mode was stable at the SA stage before significantly decreasing at the EC stage, the θ-band mode modulated in the opposite direction with a significant increase at the EC stage. Overall, the changes were much stronger at the EC stage, which was confirmed in larger groups of patients by pairwise comparisons between A and the two later stroke stages: no change was found for any of the modes when comparing the A to the SA stage (Fig. 4B(a)), whereas a strong increase and decrease in the θ and α-band modes, respectively, was found in the EC stage ($p_{Bonf} < 0.05$, Fig. 4B(b)). Finally, no significant modulation of the β-band mode through stroke stages was found in any of the tensor decompositions.

Modulation of brain oscillatory modes as a proxy of motor recovery

We further explored the modulation across stroke stages by distinguishing patients who actually recovered along the evaluated stroke stages (recovering group) from patients who maintained stable motor functions since their inclusion at the A stage (stable group, for group definitions please see *Materials and Methods*). The two groups drastically diverged regarding the modulation across stroke stages. These data indicate that the previously observed modulations were mainly driven by the recovering group, in which the same significant effects were observed between SA and EC stages ($p_{Bonf} < 0.05$; Fig. 5A, right), whereas no change was noticeable within the stable group between stroke stages (Fig. 5A, left).

All tensor decompositions showed variability in the weights of modes among patients, i.e., within the 4th dimension. We next aimed to explain the variability among patients in terms of impairment, function and recovery, by linking this variability with the different modes and their changes (Fig. 5B). No statistical evidence was found for either a link or an absence of links between θ- and β-band modes on motor scores all $1/3 < BF_{10} < 3$) in any of the tested patient cohorts. However, moderate to strong statistical evidence was found for a link between the α-band mode and motor scores in the A stage and its evolution across the SA and EC stages in the recovering group. First, patients who exhibited a stronger weight associated with this α-band mode were more impaired in the A stage (Fig. 5B(a)), with lower FM hand scores (τ = [-0.09 -0.7], BF_{10} = 7.3). Broader associations with the α-mode were found in better recovering patients between the A and SA stages (Fig. 5B(b)), as revealed by a stronger change ratio between the A and SA stages in the FM hand (τ = [0.22 0.8], BF_{10} = 91; BF_{10} = 6.5 when controlling for the initial level of impairment), wrist (τ = [0.05 0.65], BF_{10} = 3.9), and UL scores (τ = [0.07 0.67], BF_{10} = 5.8) as well as the maximum fist force (τ = [0.07 0.67], BF_{10} = 5.9). The stronger the patients were associated to this α-band

mode, the better they improved at the SA stage. Finally, a similar association was found in the longer term, with stronger change ratios between the A and EC stages in scores on the FM hand (τ = [0.2 0.8], BF_{10} = 56; BF_{10} = 12 when controlling for the initial level of impairment), BnB (τ = [0.08 0.7], BF_{10} = 6.0) and nine-hole peg tests (τ = [-0.08 -0.7], BF_{10} = 6.0) (Fig. 5B(c)), indicating that greater changes in the α-band mode were associated with larger improvements in motor functions and thus larger reductions in impairment.

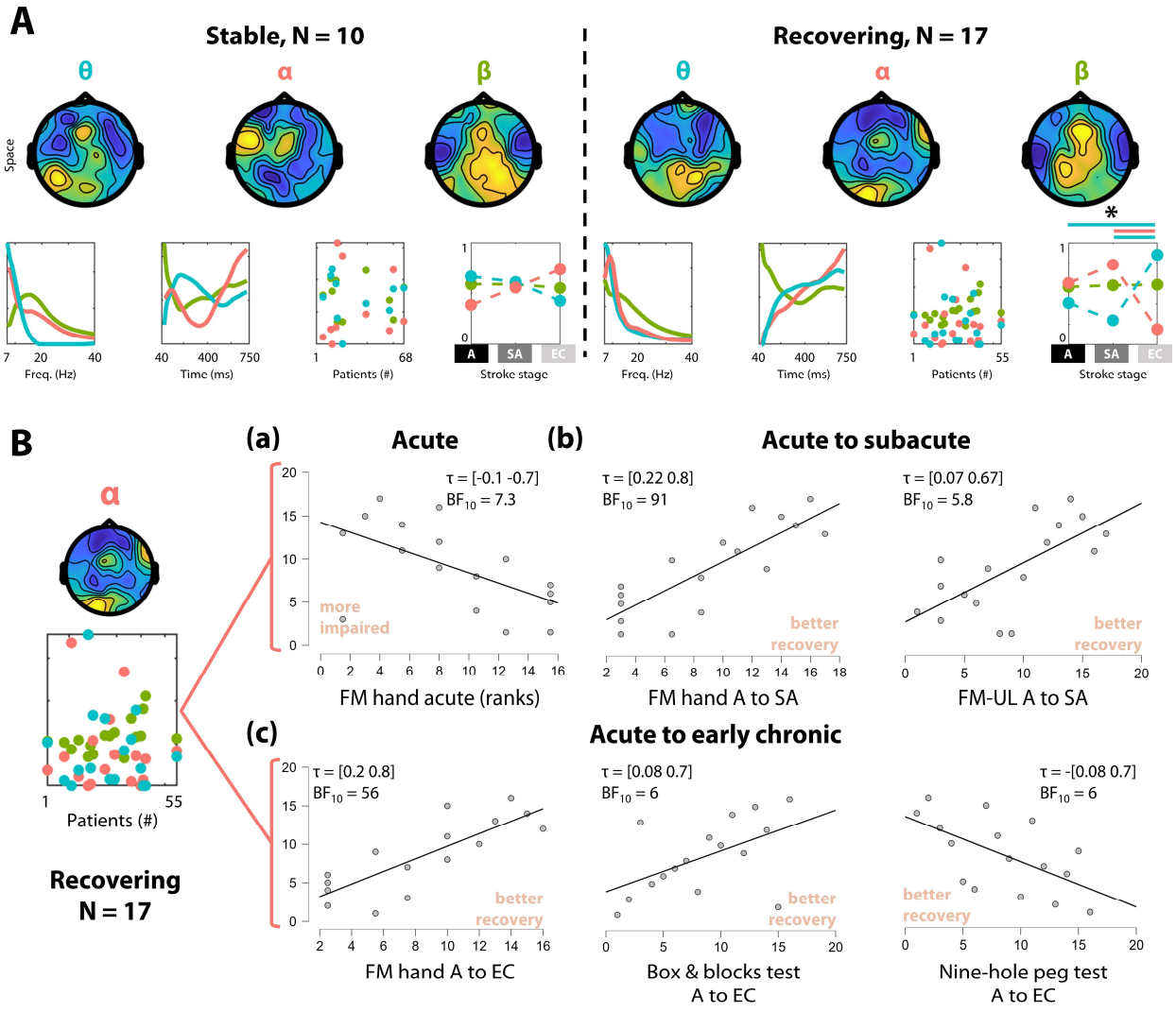

Fig. 5. Links among brain oscillatory modes, motor impairment and motor recovery. (**A**). PARAFAC decomposition of the 5D tensor in stable (left) and recovering (right) patients (see Fig. 3). (**B**) Association between the α-band mode and motor scores (FM and performance on the box & block and nine-hole peg tests) in the recovering group. The Kendall rank correlation coefficient (τ) and Bayesian factors (BF_{10}) are

indicated for each comparison, and all data are plotted according to their rank (see *Statistical analysis*). (**a**). Moderate evidence of an anticorrelation between α-band mode and motor impairment in the acute stage indicates that a more positive α-band mode in the acute stage led to more impairment. (**b**). Moderate to strong evidence of a correlation between α-band mode and changes in motor impairment to the subacute stage indicates that the greater the change in the α-band mode, the larger the reduction in impairment. (**c**). Moderate to strong evidence of correlations between α-band mode and changes in motor functions and impairment to the early-chronic stage indicate that the greater the change in the α-band mode, the better the improvement in motor functions, and the larger the reduction in impairment.

DISCUSSION

In the present study, we report longitudinal changes in induced oscillatory activity associated with functional motor recovery in a large cohort of stroke patients. The results, together with other current work*(40)*, highlight dynamic changes in correlates of inhibitory activity towards a recovery-supporting disinhibition from the subacute to the early chronic stage (for a schematic summary please see Fig. 6).

The evolution of TMS-induced oscillations might be a relevant proxy of functional reorganization and its underlying mechanisms. On the one hand, as θ oscillations are an important basis for interregional communication *(29–31)*, their positive modulation during recovery might be the signature of the re-establishment of large-scale functional connectivity within the motor network to foster functional recovery (Fig. 4). Growing evidence suggests that stroke has a direct impact on functional connectivity *(2)*, i.e., neural communication within connected brain areas. The disturbance of functional connectivity has been associated with proportional neurological deficits in stroke patients (see, e.g., *(61-63)*), and normalization of functional connectivity over time is linked with recovery (e.g., *(52, 53)*. Even though the increase in the θ oscillatory mode observed in the early chronic stage was not directly linked with motor scores, this increase was observable when recovering patients were included in the data tensor, indicating normalization of

interregional interactions (Fig. 5A). On the other hand, the longitudinal decrease observed in the α mode, together with the absence of any significant change within the β-band mode, may underline the importance of the evolution of the excitatory/inhibitory balance across stroke stages (Fig. 4). As TMS-induced alpha and beta-band activity has been linked with the GABAergic *(23)* and glutamatergic *(26)* systems respectively, our results rather pointed to a dominantly GABAergic activity changing compared to glutamatergic activity. This finding points to the existence of a beneficial disinhibition phase, especially in the recovering patient group.

The α-band modulations found here can thus be considered a proxy of the dynamic evolution of the intracortical inhibitory system *(23)*, which has been suggested to sustain motor recovery *(28, 71)*. Immediately after stroke, during the hyperacute phase, hyperinhibition of the perilesional cortical areas prevents additional tissue damage due to ischemia-induced excitotoxicity *(55–57)*. However, the persistence of hyperinhibition over time was correlated with worse motor outcomes *(27, 28)*, and pharmacological reduction in GABAergic inhibition led to better recovery in animal models *(9, 58, 59)*. Further evidence has confirmed this last point by linking better motor recovery with a period of plasticity driven by molecular changes, such as cellular excitability *(60)*, or by sustained disinhibition during the first weeks poststroke. Moreover, the existence of this beneficial disinhibition stage is also confirmed in the present cohort of patients when specifically studying cortical reactivity*(40)*. Our results showed that an abnormally stronger reactivity, supported by intracortical motor disinhibition assessed via paired-pulse TMS, was linked with better motor outcome. Overall, this disinhibition has been suggested to promote functional reorganization within the lesioned hemisphere *(54, 55, 61)*. Consistent with this suggestion, the decrease in the α-band mode in the recovering patient group is most likely a correlate of the disinhibition between

the subacute and early chronic stages (three weeks to three months poststroke), which supports the recovery process (please see Fig. 6 for a schematic).

The time frame of this phenomenon is somewhat delayed compared with our findings regarding brain reactivity on the present cohort*(40)* and the previous findings of Liuzzi *et al. (28)*, in which disinhibition occurred from the first days to up to three weeks after stroke onset. The slight differences in the precise timing of this effect might stem from the brain areas and networks represented by the specific measures and the specific temporal windows from which they are extracted. The electrical activation of neuronal populations subsequent to the TMS pulse is first spatially restricted to the targeted cortical site, before propagating along white matter pathways to reach distant cortical and subcortical sites (see, e.g. *(62)*). Then, while the short-interval intracortical inhibition protocol used in our study*(40)* and by Liuzzi *et al. (28)* allows measurement of the intracortical GABAergic activity locally within the motor cortex, the late induced α oscillations in the present work are linked with inhibitory activity at a more global scale, i.e., engaged in higher-order processes within larger-scale brain networks (Fig. 6). The disinhibition phenomenon might first occur locally within the lesioned motor cortex in the acute to subacute stage before spreading to a larger number of areas to promote functional plasticity more broadly and thus support more complex motor functions in later stages, as revealed here by the later association with improvement in complex motor tasks such as BnB and 9HP. Finally, the absence of change in α activity in stable patients might be the signature of the normalization of inhibitory activity. In this patient group, a beneficial disinhibition phase might have already occurred earlier and transiently, explaining their stable and high motor function upon their inclusion in the study.

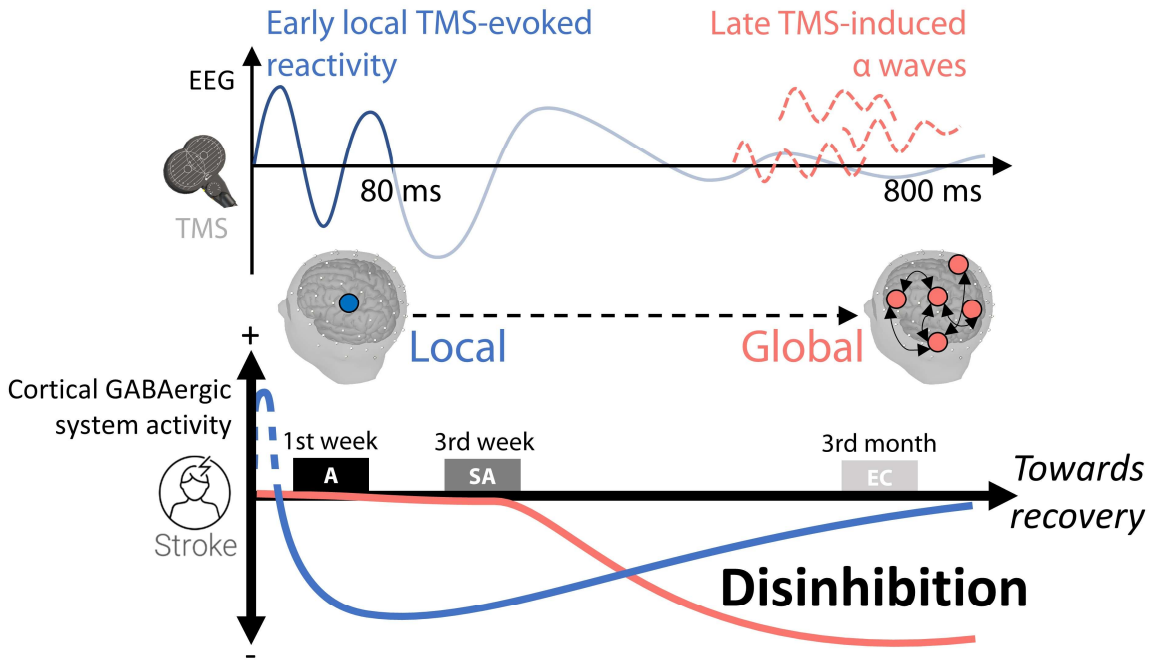

Fig. 6. Time course of GABAergic inhibition and its relationship with recovery. The changes in early TMS-evoked reactivity (as demonstrated in Harquel *et al.*, 2023 *(40)*) and in late TMS-induced α waves, both most likely correlates of a decrease in GABAergic activity at different spatial scales, represent recovery-facilitating functional disinhibition after the detrimental hyper-inhibitory period in the hyper-acute stage after the stroke. Based on the present findings, this disinhibition occurs in two phases: first locally within the ipsilesional motor cortex in the acute to subacute stage, and then more broadly toward the early chronic stage. Such disinhibition fosters structural and functional plasticity that support motor recovery *(54, 55, 61)*.

Limitations

Despite the exciting opportunities that the present analytical method provides, there are a few limitations worth mentioning, namely, the lack of a sham stimulation condition, and the variation in the patient cohort. Recent guidelines about TMS-EEG coupling acquisition and data processing were followed in this work, with the exception of the presence of a realistic sham stimulation condition in order to assess the influence of peripheral evoked potentials, due to the multisensory features of TMS, on the recorded EEG signal *(63, 64)*. However, since the present work is based on TMS-induced oscillations, which are computed after removing such evoked components from

the signal, and on a longitudinal analysis approach, the lack of a sham stimulation condition does not relevantly affect the interpretation of the results. Finally, the distribution of the patient cohort with respect to the severity of motor impairment in the acute stage was rather on the moderately to mildly impaired side. Additional analyses of more heterogeneous groups in the future will help to refine the present conclusions regarding the link between changes in brain oscillatory modes and motor recovery.

Conclusion

In summary, examining a larger cohort of stroke patients over time using TMS-induced activity provided a better understanding of the neural mechanisms linked to motor recovery. The present results support cortical disinhibition with different topographies and temporal course as an important underlying mechanism driving motor recovery between the subacute and early chronic stage. The acquired knowledge might pave the way for developing novel biomarkers to determine and predict stroke recovery and to personalize innovative therapies based on modulation of brain oscillatory activity through noninvasive or invasive brain stimulation technologies.

ACKNOWLEGMENTS

We thank the MRI and neuromodulation facilities of the Human Neuroscience Platform of the Fondation Campus Biotech Geneva and the Neuroimaging Center of the Sion Hospital and the Center for Biomedical Imaging, a Swiss research center of excellence, for their expertise and access to their facilities.

FUNDING

This work was supported by grants from the 'Personalized Health and Related Technologies (PHRT-#2017-205)' of the ETH Domain (CH), the Defitech Foundation (Strike-the-Stroke project, Morges, CH), the SNSF (NIBS-iCog, 320030L_197899 / 1) and the Wyss Center for Bio- and Neuroengineering (WP030; Geneva, CH).

COMPETITING INTERESTS

The authors report that they have no competing interests.

AUTHOR CONTRIBUTIONS

Conceptualization: SH, ACM, TM, DvdV, MJW, PK, and FCH

Methodology: SH, ACM, TM, MW, and FCH

Investigation: SH, ACM, TM, LF, MC, PM, JB, NM, EB, JA, CJ, AM, CC, VA, PV, JAG, JLT, DSM, CB, PJK, and MJD

Visualization: SH and ACM

Funding acquisition: FCH, DvdV, OB, and SM

Project administration: FCH, TM, MJW, and PJK

Supervision: FCH, PJK, MJW, and TM

Writing – original draft: SH

Writing – review & editing: all authors

REFERENCES

1. C. Grefkes, G. R. Fink, Recovery from stroke: current concepts and future perspectives. *Neurol Res Pract* **2**, 17 (2020).

2. A. G. Guggisberg, P. J. Koch, F. C. Hummel, C. Buetefisch, Brain networks and their relevance for stroke rehabilitation. *Clin Neurophysiol* **130**, 1098–1124 (2019).

3. E. Raffin, F. C. Hummel, Restoring Motor Functions After Stroke: Multiple Approaches and Opportunities. *Neuroscientist* **24**, 400–416 (2018).

4. D. Smajlović, Strokes in young adults: epidemiology and prevention. *Vasc Health Risk Manag* **11**, 157–164 (2015).

5. M. Coscia, M. J. Wessel, U. Chaudary, J. D. R. Millán, S. Micera, A. Guggisberg, P. Vuadens, J. Donoghue, N. Birbaumer, F. C. Hummel, Neurotechnology-aided interventions for upper limb motor rehabilitation in severe chronic stroke. *Brain* **142**, 2182–2197 (2019).

6. P. J. Koch, F. C. Hummel, Toward precision medicine: tailoring interventional strategies based on noninvasive brain stimulation for motor recovery after stroke. *Current Opinion in Neurology* **30**, 388–397 (2017).

7. S. Micera, M. Caleo, C. Chisari, F. C. Hummel, A. Pedrocchi, Advanced Neurotechnologies for the Restoration of Motor Function. *Neuron* **105**, 604–620 (2020).

8. J. Cirillo, R. A. Mooney, S. J. Ackerley, P. A. Barber, V. M. Borges, A. N. Clarkson, C. Mangold, A. Ren, M.-C. Smith, C. M. Stinear, W. D. Byblow, Neurochemical balance and inhibition at the subacute stage after stroke. *J Neurophysiol* **123**, 1775–1790 (2020).

9. A. N. Clarkson, B. S. Huang, S. E. MacIsaac, I. Mody, S. T. Carmichael, Reducing excessive GABA-mediated tonic inhibition promotes functional recovery after stroke. *Nature* **468**, 305–309 (2010).

10. S. T. Carmichael, Brain excitability in stroke: the yin and yang of stroke progression. *Arch Neurol* **69**, 161–167 (2012).

11. G. Liuzzi, V. Horniss, P. Lechner, J. Hoppe, K. Heise, M. Zimerman, C. Gerloff, F. C. Hummel, Development of movement-related intracortical inhibition in acute to chronic subcortical stroke. *Neurology* **82**, 198–205 (2014).

12. F. C. Hummel, B. Steven, J. Hoppe, K. Heise, G. Thomalla, L. G. Cohen, C. Gerloff, Deficient intracortical inhibition (SICI) during movement preparation after chronic stroke. *Neurology* **72**, 1766–1772 (2009).

13. J. U. Blicher, J. Near, E. Næss-Schmidt, C. J. Stagg, H. Johansen-Berg, J. F. Nielsen, L. Østergaard, Y.-C. L. Ho, GABA levels are decreased after stroke and GABA changes during rehabilitation correlate with motor improvement. *Neurorehabil Neural Repair* **29**, 278–286 (2015).

14. P. Julkunen, V. K. Kimiskidis, P. Belardinelli, Bridging the gap: TMS-EEG from lab to clinic. *Journal of Neuroscience Methods* **369**, 109482 (2022).

15. J. C. Hernandez-Pavon, D. Veniero, T. O. Bergmann, P. Belardinelli, M. Bortoletto, S. Casarotto, E. P. Casula, F. Farzan, M. Fecchio, P. Julkunen, E. Kallioniemi, P. Lioumis, J. Metsomaa, C. Miniussi, T. P. Mutanen, L. Rocchi, N. C. Rogasch, M. M. Shafi, H. R. Siebner, G. Thut, C. Zrenner, U. Ziemann, R. J. Ilmoniemi, TMS combined with EEG: Recommendations and open issues for data collection and analysis. *Brain Stimulation* (2023), doi:10.1016/j.brs.2023.02.009.

16. B. Passera, A. Chauvin, E. Raffin, T. Bougerol, O. David, S. Harquel, Exploring the spatial resolution of TMS-EEG coupling on the sensorimotor region. *NeuroImage* **259**, 119419 (2022).

17. V. Moliadze, Y. Zhao, U. Eysel, K. Funke, Effect of transcranial magnetic stimulation on single-unit activity in the cat primary visual cortex. *The Journal of Physiology* **553**, 665–679 (2003).

18. M. C. Pellicciari, D. Veniero, C. Miniussi, Characterizing the Cortical Oscillatory Response to TMS Pulse. *Front Cell Neurosci* **11**, 38 (2017).

19. S. Harquel, T. Bacle, L. Beynel, C. Marendaz, A. Chauvin, O. David, Mapping dynamical properties of cortical microcircuits using robotized TMS and EEG: Towards functional cytoarchitectonics. *Neuroimage* **135**, 115–124 (2016).

20. M. Rosanova, A. Casali, V. Bellina, F. Resta, M. Mariotti, M. Massimini, Natural Frequencies of Human Corticothalamic Circuits. *Journal of Neuroscience* **29**, 7679–7685 (2009).

21. M. C. Pellicciari, S. Bonnì, V. Ponzo, A. M. Cinnera, M. Mancini, E. P. Casula, F. Sallustio, S. Paolucci, C. Caltagirone, G. Koch, Dynamic reorganization of TMS-evoked activity in subcortical stroke patients. *NeuroImage* **175**, 365–378 (2018).

22. T. Mutanen, TMS-evoked changes in brain-state dynamics quantified by using EEG data. *Frontiers in Human Neuroscience* **7** (2013), doi:10.3389/fnhum.2013.00155.

23. I. Premoli, T. O. Bergmann, M. Fecchio, M. Rosanova, A. Biondi, P. Belardinelli, U. Ziemann, The impact of GABAergic drugs on TMS-induced brain oscillations in human motor cortex. *NeuroImage* **163**, 1–12 (2017).

24. R. A. Harshman, FOUNDATIONS OF THE PARAFAC PROCEDURE: MODELS AND CONDITIONS FOR AN "EXPLANATORY" MULTIMODAL FACTOR ANALYSIS. , 84.

25. C. Tangwiriyasakul, I. Premoli, L. Spyrou, R. F. Chin, J. Escudero, M. P. Richardson, Tensor decomposition of TMS-induced EEG oscillations reveals data-driven profiles of antiepileptic drug effects. *Sci Rep* **9**, 17057 (2019).

26. P. Belardinelli, F. König, C. Liang, I. Premoli, D. Desideri, F. Müller-Dahlhaus, P. C. Gordon, C. Zipser, C. Zrenner, U. Ziemann, TMS-EEG signatures of glutamatergic neurotransmission in human cortex. *Sci Rep* **11**, 8159 (2021).

27. M. Bortoletto, D. Veniero, G. Thut, C. Miniussi, The contribution of TMS–EEG coregistration in the exploration of the human cortical connectome. *Neuroscience & Biobehavioral Reviews* **49**, 114–124 (2015).

28. H. R. Siebner, K. Funke, A. S. Aberra, A. Antal, S. Bestmann, R. Chen, J. Classen, M. Davare, V. Di Lazzaro, P. T. Fox, M. Hallett, A. N. Karabanov, J. Kesselheim, M. Malling Beck, G. Koch, D. Liebetanz, S. Meunier, C. Miniussi, W. Paulus, A. V. Peterchev, T. Popa, M. C. Ridding, A. Thielscher, U. Ziemann, J. C. Rothwell, Y. Ugawa, Transcranial magnetic stimulation of the brain: What is stimulated? – a consensus and critical position paper. *Clinical Neurophysiology* (2022), doi:10.1016/j.clinph.2022.04.022.

29. R. T. Canolty, E. Edwards, S. S. Dalal, M. Soltani, S. S. Nagarajan, H. E. Kirsch, M. S. Berger, N. M. Barbaro, R. T. Knight, High gamma power is phase-locked to theta oscillations in human neocortex. *Science* **313**, 1626–1628 (2006).

30. E. A. Solomon, J. E. Kragel, M. R. Sperling, A. Sharan, G. Worrell, M. Kucewicz, C. S. Inman, B. Lega, K. A. Davis, J. M. Stein, B. C. Jobst, K. A. Zaghloul, S. A. Sheth, D. S. Rizzuto, M. J. Kahana, Widespread theta synchrony and high-frequency desynchronization underlies enhanced cognition. *Nat Commun* **8**, 1704 (2017).

31. A. J. Watrous, N. Tandon, C. R. Conner, T. Pieters, A. D. Ekstrom, Frequency-specific network connectivity increases underlie accurate spatiotemporal memory retrieval. *Nat Neurosci* **16**, 349–356 (2013).

32. Z. Keser, S. C. Buchl, N. A. Seven, M. Markota, H. M. Clark, D. T. Jones, G. Lanzino, R. D. Brown, G. A. Worrell, B. N. Lundstrom, Electroencephalogram (EEG) With or Without Transcranial Magnetic Stimulation (TMS) as Biomarkers for Post-stroke Recovery: A Narrative Review. *Front. Neurol.* **13**, 827866 (2022).

33. F. Hummel, F. Andres, E. Altenmüller, J. Dichgans, C. Gerloff, Inhibitory control of acquired motor programmes in the human brain. *Brain* **125**, 404–420 (2002).

34. O. Jensen, A. Mazaheri, Shaping Functional Architecture by Oscillatory Alpha Activity: Gating by Inhibition. *Frontiers in Human Neuroscience* **4** (2010) (available at https://www.frontiersin.org/article/10.3389/fnhum.2010.00186).

35. W. Klimesch, P. Sauseng, S. Hanslmayr, EEG alpha oscillations: the inhibition-timing hypothesis. *Brain Res Rev* **53**, 63–88 (2007).

36. G. Pfurtscheller, A. Stancák, C. Neuper, Event-related synchronization (ERS) in the alpha band--an electrophysiological correlate of cortical idling: a review. *Int J Psychophysiol* **24**, 39–46 (1996).

37. P. Sauseng, W. Klimesch, K. F. Heise, W. R. Gruber, E. Holz, A. A. Karim, M. Glennon, C. Gerloff, N. Birbaumer, F. C. Hummel, Brain oscillatory substrates of visual short-term memory capacity. *Curr Biol* **19**, 1846–1852 (2009).

38. G. Thut, A. Nietzel, S. A. Brandt, A. Pascual-Leone, Alpha-band electroencephalographic activity over occipital cortex indexes visuospatial attention bias and predicts visual target detection. *J Neurosci* **26**, 9494–9502 (2006).

39. L. Fleury, P. J. Koch, M. J. Wessel, C. Bonvin, D. S. Millan, C. Constantin, P. Vuadens, J. Adolphsen, A. G. Cadic-Melchior, J. Brügger, E. Beanato, M. Ceroni, P. Menoud, D. de L. Rodriguez, V. Zufferey, N. Meyer, P. Egger, S. Harquel, T. Popa, E. Raffin, G. Girard, J. P. Thiran, C. Vaney, V. Alvarez, J.-L. Turlan, A. Mühl, B. Leger, T. Morishita, S. Micera, O. Blanke, D. V. de Ville, F. C. Hummel, Towards individualized Medicine in Stroke – the TiMeS project: protocol of longitudinal, multi-modal, multi-domain study in stroke, 2022.05.18.22274612 (2022).

40. A. Cadic-Melchior, S. Harquel, T. Morishita, L. Fleury, A. Witon, M. Ceroni, J. Bruegger, N. Meyer, G. Evangelista, P. Egger, E. Beanato, P. Menoud, D. V. D. Ville, S. Micera, O. Blanke, B. Leger, J. Adolphsen, C. Jagella, C. Constantin, V. Alvarez, P. Vuadens, J.-A. Ghika, J.-L. Turlan, A. Muhl, D. S. Millan, C. Bonvin, P. J. Koch, M. Wessel, F. C. Hummel, Stroke recovery related changes in brain reactivity based on modulation of intracortical inhibition, 2022.09.20.22280144 (2022).

41. A. R. Fugl-Meyer, L. Jääskö, I. Leyman, S. Olsson, S. Steglind, A method for evaluation of physical performance. *Scand J Rehabil Med* **7**, 13–31 (1975).

42. V. Mathiowetz, G. Volland, N. Kashman, K. Weber, Adult norms for the Box and Block Test of manual dexterity. *The American journal of occupational therapy* **39**, 386–391 (1985).

43. A. Delorme, S. Makeig, EEGLAB: an open source toolbox for analysis of single-trial EEG dynamics including independent component analysis. *Journal of neuroscience methods* **134**, 9–21 (2004).

44. N. C. Rogasch, C. Sullivan, R. H. Thomson, N. S. Rose, N. W. Bailey, P. B. Fitzgerald, F. Farzan, J. C. Hernandez-Pavon, Analysing concurrent transcranial magnetic stimulation and electroencephalographic data: A review and introduction to the open-source TESA software. *Neuroimage* **147**, 934–951 (2017).

45. N. C. Rogasch, R. H. Thomson, F. Farzan, B. M. Fitzgibbon, N. W. Bailey, J. C. Hernandez-Pavon, Z. J. Daskalakis, P. B. Fitzgerald, Removing artefacts from TMS-EEG recordings using independent component analysis: Importance for assessing prefrontal and motor cortex network properties. *NeuroImage* **101**, 425–439 (2014).

46. R. Oostenveld, P. Fries, E. Maris, J.-M. Schoffelen, FieldTrip: Open Source Software for Advanced Analysis of MEG, EEG, and Invasive Electrophysiological Data. *Computational Intelligence and Neuroscience* **2011**, 1–9 (2011).

47. M. X. Cohen, T. H. Donner, Midfrontal conflict-related theta-band power reflects neural oscillations that predict behavior. *Journal of Neurophysiology* **110**, 2752–2763 (2013).

48. H. Jeffreys, *The Theory of Probability* (OUP Oxford, 1998).

49. M. A. Urbin, X. Hong, C. E. Lang, A. R. Carter, Resting-state functional connectivity and its association with multiple domains of upper-extremity function in chronic stroke. *Neurorehabil Neural Repair* **28**, 761–769 (2014).

50. M. Allegra, C. Favaretto, N. Metcalf, M. Corbetta, A. Brovelli, Stroke-related alterations in inter-areal communication. *Neuroimage Clin* **32**, 102812 (2021).

51. A. R. Carter, S. V. Astafiev, C. E. Lang, L. T. Connor, J. Rengachary, M. J. Strube, D. L. W. Pope, G. L. Shulman, M. Corbetta, Resting interhemispheric functional magnetic resonance imaging connectivity predicts performance after stroke. *Ann Neurol* **67**, 365–375 (2010).

52. A.-M. Golestani, S. Tymchuk, A. Demchuk, B. G. Goodyear, VISION-2 Study Group, Longitudinal evaluation of resting-state FMRI after acute stroke with hemiparesis. *Neurorehabil Neural Repair* **27**, 153–163 (2013).

53. J. Wu, E. B. Quinlan, L. Dodakian, A. McKenzie, N. Kathuria, R. J. Zhou, R. Augsburger, J. See, V. H. Le, R. Srinivasan, S. C. Cramer, Connectivity measures are robust biomarkers of cortical function and plasticity after stroke. *Brain* **138**, 2359–2369 (2015).

54. R. A. Mooney, S. J. Ackerley, D. K. Rajeswaran, J. Cirillo, P. A. Barber, C. M. Stinear, W. D. Byblow, The Influence of Primary Motor Cortex Inhibition on Upper Limb Impairment and Function in Chronic Stroke: A Multimodal Study. *Neurorehabil Neural Repair* **33**, 130–140 (2019).

55. A. N. Clarkson, B. S. Huang, S. E. Macisaac, I. Mody, S. T. Carmichael, Reducing excessive GABA-mediated tonic inhibition promotes functional recovery after stroke. *Nature* **468**, 305–309 (2010).

56. G. Michalettos, K. Ruscher, Crosstalk Between GABAergic Neurotransmission and Inflammatory Cascades in the Post-ischemic Brain: Relevance for Stroke Recovery. *Front Cell Neurosci* **16**, 807911 (2022).

57. R. G, H. Jw, N. Y, W. A, L. J, Perturbation of Brain Oscillations after Ischemic Stroke: A Potential Biomarker for Post-Stroke Function and Therapy. *International journal of molecular sciences* **16** (2015), doi:10.3390/ijms161025605.

58. R. Lamtahri, M. Hazime, E. K. Gowing, R. Y. Nagaraja, J. Maucotel, M. Alasoadura, P. P. Quilichini, K. Lehongre, B. Lefranc, K. Gach-Janczak, A.-B. Marcher, S. Mandrup, D. Vaudry, A. N. Clarkson, J. Leprince, J. Chuquet, The Gliopeptide ODN, a Ligand for the Benzodiazepine Site of GABAA Receptors, Boosts Functional Recovery after Stroke. *J Neurosci* **41**, 7148–7159 (2021).

59. F. Lebrun, N. Violle, A. Letourneur, C. Muller, N. Fischer, A. Levilly, C. Orset, A. Sors, D. Vivien, Post-acute delivery of α5-GABAA antagonist, S 44819, improves functional recovery in juvenile rats following stroke. *Experimental Neurology* **347**, 113881 (2022).

60. M. T. Joy, S. T. Carmichael, Encouraging an excitable brain state: mechanisms of brain repair in stroke. *Nat Rev Neurosci* **22**, 38–53 (2021).

61. G. Liuzzi, V. Hörniß, P. Lechner, J. Hoppe, K. Heise, M. Zimerman, C. Gerloff, F. C. Hummel, Development of movement-related intracortical inhibition in acute to chronic subcortical stroke. *Neurology* **82**, 198–205 (2014).

62. D. Momi, Z. Wang, J. D. Griffiths, A. Fornito, M. J. Frank, J. Meier, A. Pigorini, Eds. TMS-evoked responses are driven by recurrent large-scale network dynamics. *eLife* **12**, e83232 (2023).

63. V. Conde, L. Tomasevic, I. Akopian, K. Stanek, G. B. Saturnino, A. Thielscher, T. O. Bergmann, H. R. Siebner, The non-transcranial TMS-evoked potential is an inherent source of ambiguity in TMS-EEG studies. *NeuroImage* **185**, 300–312 (2019).

64. P. Belardinelli, M. Biabani, D. M. Blumberger, M. Bortoletto, S. Casarotto, O. David, D. Desideri, A. Etkin, F. Ferrarelli, P. B. Fitzgerald, A. Fornito, P. C. Gordon, O. Gosseries, S. Harquel, P. Julkunen, C. J. Keller, V. K. Kimiskidis, P. Lioumis, C. Miniussi, M. Rosanova, S. Rossi, S. Sarasso, W. Wu, C. Zrenner, Z. J. Daskalakis, N. C. Rogasch, M. Massimini, U. Ziemann, R. J. Ilmoniemi, Reproducibility in TMS–EEG studies: a call for data sharing, standard procedures and effective experimental control. *Brain Stimulation* (2019), doi:10.1016/j.brs.2019.01.010.